

# Spaced-antenna aperture synthesis using an X-band active phased-array

V. Venkatesh\*, K. Orzel \*, S. Frasier\*

\* University of Massachusetts, Amherst, MA.

## Abstract—

Spaced antenna (SA) radars retrieve wind-fields by tracking resolution volume sized bins of scatterers as they advect between two physically displaced antennas. To date, SA methods have been applied for profiling the ionosphere and precipitation free atmosphere [1][2][3]. The primary technological difficulty in applying these methods to probe precipitation at microwave frequencies is the requirement for such a short antenna separation that a significant overlap in apertures is necessary. In this work, we synthesize overlapped apertures by segmenting active phased-arrays into sub-arrays that are multiplexed in time. Antenna pattern measurements are then employed to evaluate beamforming errors on a family of implementations. Based on measurements and Monte-Carlo simulations, we find that highly overlapping apertures are most immune to beam squint errors. This is because element-level phase errors are retained on the synthesized spaced antennas and differential beam squint errors are minimized. Finally, we demonstrate a novel method to measure relative phase center displacement between spaced antennas from weather echo statistics that obviates the need for near-field antenna measurements.

**Index Terms**—phased array, spaced antenna, x-band radar.

## I. INTRODUCTION

Spaced antenna (SA) radars correlate received signals from two displaced apertures to retrieve the wind-field component along the baseline. This SA technique for cross-beam wind measurement has been routinely employed for ionospheric sounding and profiling refractive index turbulence in the atmospheric boundary layer [1][2][3]. The low radar frequencies in these applications allowed for baselines that were relatively large in comparison to the antenna dimension. This is because the correlation time of the backscattered signal is inversely proportional to radar frequency. Long correlation times in turn allowed for long baselines.

The “see-saw” relationship between radar frequency and baseline makes the design parameters for SA weather radars at microwave frequencies challenging. SA weather radars must have a short baseline and significantly overlapping apertures to sample the spatial fading pattern before significant decorrelation occurs. If methods to synthesize closely spaced apertures with sufficient isolation are developed, the SA method may potentially allow significant improvements in the spatial resolution of wind-field retrievals. This is because existing methods

in the community such as Velocity-Azimuth-Display (VAD) rely on the scanning capability of weather radars to retrieve the large scale wind-field over a 360 degree azimuthal swath, while the SA method measures the local wind-field within a single resolution cell.

Previous schemes to implement overlapping apertures for spaced antenna weather radars employed polarization diversity to isolate antennas [4] and a passive phased-array antenna system in a monopulse configuration [5][6]. The first approach relied upon separable yet well correlated scattering of orthogonal polarizations by hydrometeors. For this dual-polarized spaced antenna (DPSA) system design, a low duty cycle transmitter restricted the pulse repetition frequency to be too small to adequately sample the correlation function. But more importantly, the mechanical motion of the beam complicated retrieval of cross-beam wind fields.

The National Weather Radar Testbed (NWRT) overcame difficulties due to mechanical scanning by employing a passive phased-array aperture. For the spaced-antenna implementation on the NWRT [5], equally dividing the array face into left and right receive sub-arrays resulted in a baseline that was so long that hydrometeor reshuffling in the resolution volume degraded retrieval precision. Although this was an important step towards realizing spaced antenna weather radars, the fixed monopulse configuration provided little means to further optimize for spaced-antenna retrievals.

To date, literature on applying the spaced-antenna method to precipitation has focused on improving models of the correlation function to account for the independent motion of hydrometeors in the resolution volume [5][6] and idealized retrieval studies based on simulations [7]. This work focuses on spaced antenna weather radar aperture synthesis using an X-band active phased array. Active phased arrays offer more flexibility in aperture synthesis, but are more sensitive to errors in beamforming. The following section outlines the design specifics of the active phased array spaced-antenna system. Based on measurements and simulations, we then evaluate errors in RF beamforming on differently sized spaced-antenna sub-arrays.

## II. ACTIVE PHASED-ARRAY SPACED-ANTENNA CONCEPT

The X-band “phase-tilt” radar system was developed by a team of engineers from the Microwave Remote Sensing Lab (MIRSL) at the University of Massachusetts [8] and the center for Collaborative and Adaptive Sensing of the

This work was performed at the University of Massachusetts. At the time of submission of this work, the corresponding author is with Jet Propulsion Laboratory, California Institute of Technology, CA. Corresponding author Email : vijay.venkatesh@jpl.nasa.gov .

Atmosphere (CASA) [9]. This system comprises of a linear array antenna, programmable Transmit/Receive modules, a master FPGA controller and a host computer. The antenna array consists of 64 “stick” elements, where each “stick” is a series-fed microstrip patch array. The full array has a 1.6 degree beamwidth in the azimuth plane and a 3.5 degree beamwidth in the elevation plane at broadside. Behind each antenna element, a Transmit/Receive (T/R) module provides independent amplitude and phase control. The T/R modules are synchronized by clocking signals provided by the master FPGA controller. A beam scheduling module on the host computer preloads beam sequences that are executed by the state machines residing in the FPGA.

Fig. 1 depicts the approach to implementing a spaced-antenna system on an active phased array radar. The entire array can be used upon transmit in order to maximize elemental contributions to transmit power. Alternating sub-arrays with displaced phase-centers are used on receive. The effective phase centers of the overlapped apertures are located midway between the centers of the transmit and receive apertures. Auto- and cross-correlation functions may be produced with interleaved time-series from separate portions of the array and enable retrievals of baseline wind. Many spaced-antenna system designs were implemented on the active phased-array radar system. The first family of implementations was an electronically scanned 2.6 degree spaced-antenna system. Here, a 2.1 degree aperture was employed on transmit aperture and a 4 degree aperture was employed on receive. Since both the aperture dimension and the aperture separation follow a cosine roll-off across electronic scan angle, they are compensated in order to provide near-constant values across scan-angle. This allowed fixed cross-correlation statistics as a function of scan angle and simplified interpretation. The second family of spaced-antenna systems focussed on broadside implementations and allowed further evaluation of RF beamforming errors.

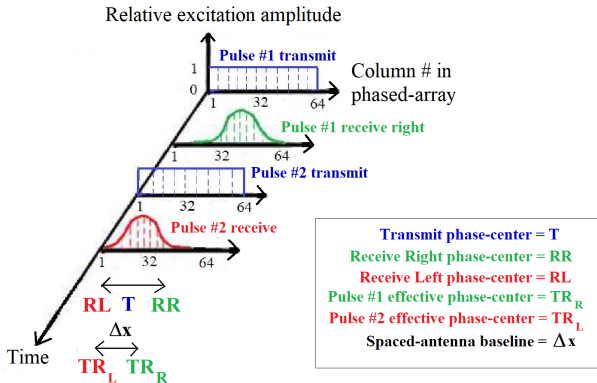


Fig. 1: Time-series of transmit/receive aperture weighting indicating left and right receive apertures interleaved with the transmit aperture. The effective spaced antenna baseline is denoted by  $\Delta x$ .

In the following section, the implemented spaced-antenna designs are evaluated in terms of three figures of merit : differences between measured and desired beamwidths, dif-

ferences between measured and desired baselines, and relative beam squint between the equivalent monostatic left and right apertures. These performance metrics are primarily synthesized from far-field pattern measurements. Where necessary, “simulated” values are used as a prognostic. These simulated values take T/R module failure into account, and add pseudo-random numbers to the desired weighting to mimic quantization errors. Rayleigh statistics for RMS amplitude errors and uniform distributions for RMS phase errors were assumed [10]. Beamwidths were then calculated from the corresponding far-field patterns assuming no mutual coupling between the elements. Further, the simple simulation methodology employed herein does not incorporate element level differences in sub-arrays such as mutual coupling and edge effects. Lastly, a novel statistical method is demonstrated to gauge the implemented baseline.

### III. APERTURE SYNTHESIS RESULTS

#### A. Beam width measurements

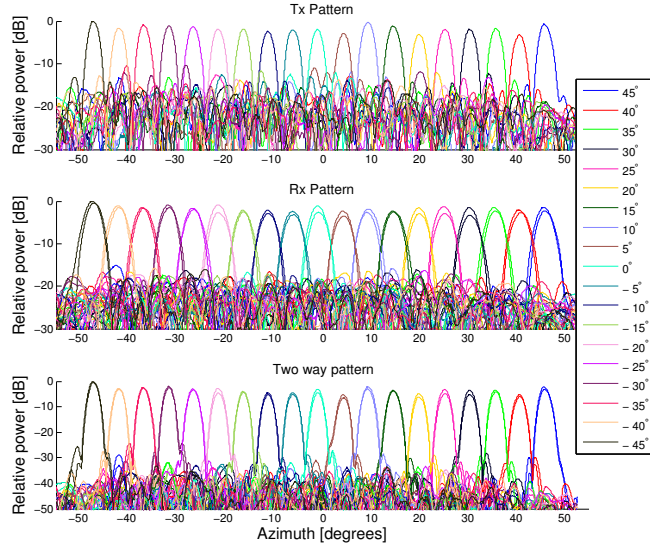


Fig. 2: Azimuthal scans of a beacon using the 2.6 degree equivalent one-way beamwidth spaced-antenna system. The patterns were measured by mechanically slewing the array face past a beacon.

Fig. 2 shows qualitative results of antenna far field measurements for the electronically scanned 2.6 degree spaced-antenna systems. Beam locations spanning  $-45$  to  $45$  degrees in steps of  $5$  degrees were implemented. The first sub-panel shows far-field patterns corresponding to the transmit beam. The second panel shows receive antenna patterns with the left and right sub-arrays overlaid for each beam location. Unlike the transmit pattern where a uniform aperture weighting resulted in sidelobes of approximately  $13$  dB, the receive pattern corresponds to a Taylor weighting applied across the sub-array and has significantly lower sidelobes. The bottom panel shows two-way patterns that are obtained by multiplying the transmit and receive patterns. As expected, the two-way

pattern corresponding to the left and right spaced-antenna apertures are similar.

Some comments about the far-field pattern measurement methodology in Fig. 2 are in order. A pyramidal horn located at a distance of 85 m from the array was used as a source for the receive patterns and as a receiver to measure transmit patterns. The radar was slowly slewed mechanically about the horn antenna, while rapid electronic scans were performed. The electronic scan was implemented as a sequence of discrete beams with a dwell time of 10 milli-seconds each. A slow mechanical slew allowed recording the power received by each beam over an azimuth span of 180 degrees. Two comments about the measurement methodology are in order. First, both the horn and the phased-array antenna system were located only several meters above ground level. This in turn left some locations vulnerable to multi-path effects in the vertical plane and limited the fidelity of gain measurements. Second, antenna pattern measurements are conventionally made rotating the aperture about its expected phase-center [10]. For the spaced-antenna sub-arrays, this was not the case and the entire array was rotated about its physical center. But given the spaced antenna baselines investigated in this work are short relative to antenna azimuth dimension, we neglect errors due to asymmetric phase centers.

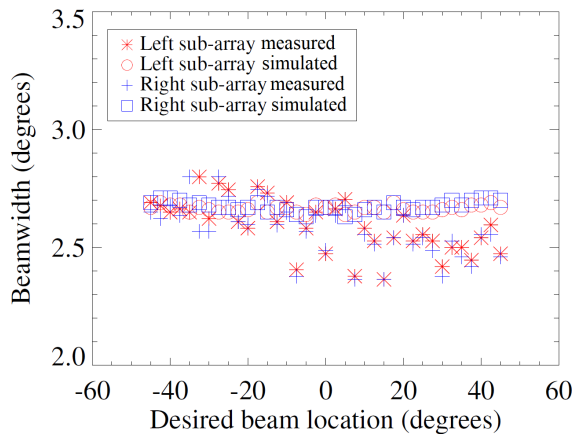


Fig. 3: Estimates of beamwidth from antenna-pattern measurements compared with corresponding simulation predictions for the implemented sub-arrays. In spite of neglecting mutual coupling and edge effects, simulations and measurements agree to first order.

Fig. 3 shows derived antenna beamwidths along with the respective expected values for the 2.6 degree arrays as a function of scan angle. Note that the spaced-antenna systems close to broadside agree best with simulations. One possible explanation for the difference in measurements and simulations away from broadside are mutual coupling effects that are neglected by the simple simulation methodology used herein. The measurements of beamwidth are also of finite precision themselves. The net result of all this is that it may be advantageous to use the Full Correlation Analysis (FCA) algorithm for subsequent spaced-antenna retrievals in electronically scanned systems. This is because the FCA algorithm does not require precise knowledge of the antenna

pattern to retrieve the baseline wind.

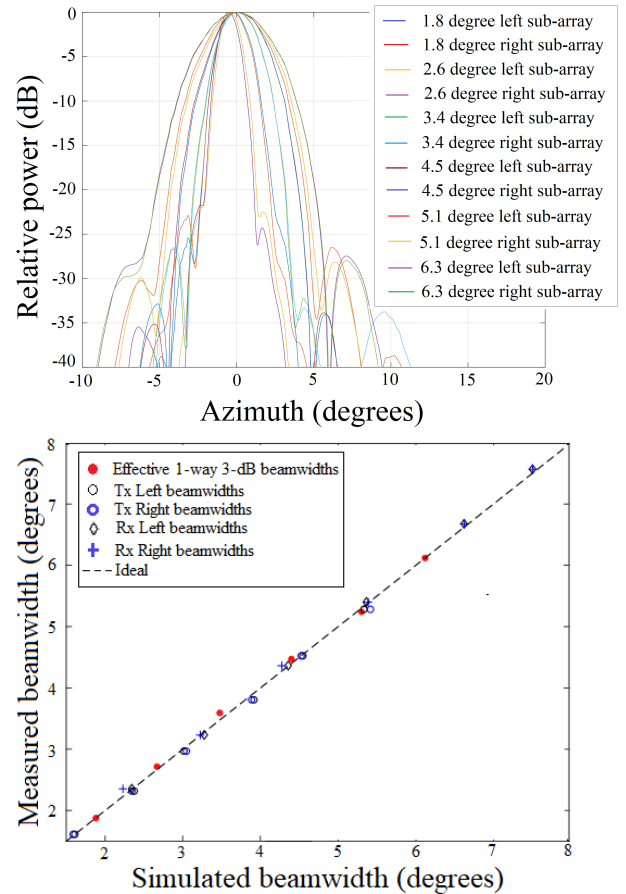


Fig. 4: Top - Effective two-way antenna patterns of spaced-antenna systems with varying sub-array sizes. The location of the beams and the shapes of the main beams only approximate desired patterns. Bottom - Beamwidths of broadside patterns for various sub-array implementations. At broadside, the sub-array implementations are in much better agreement with simulations.

Fig. 4 shows far-field pattern measurements of two-way antenna patterns synthesized for spaced-antenna sub-arrays at broadside. Some differences between the left and right synthesized beams are noticeable. As a practical matter, it is difficult to distinguish between systematic and random errors on sub-arrays using one measurement of the phased-array antenna system. For example, the residual errors in T/R module path phase compensation may have different statistics over short and long spatial scales. These errors may change over time. The net effect of all this is that it is more convenient to correct for beamforming errors in the retrieval process where possible, than to attempt to eliminate amplitude and phase errors completely. Notwithstanding, the left and right spaced antenna patterns appear matched to first order and the sidelobe levels are better than 20 dB. Furthermore, the bottom panel shows that beamwidths synthesized from the measurements agree well with simulations. Note that the simulations used herein neglect mutual coupling effects. As a consequence, the agreement between simulations and

measurements is significantly better at broadside, as compared to higher scan angles.

### B. Baseline measurements

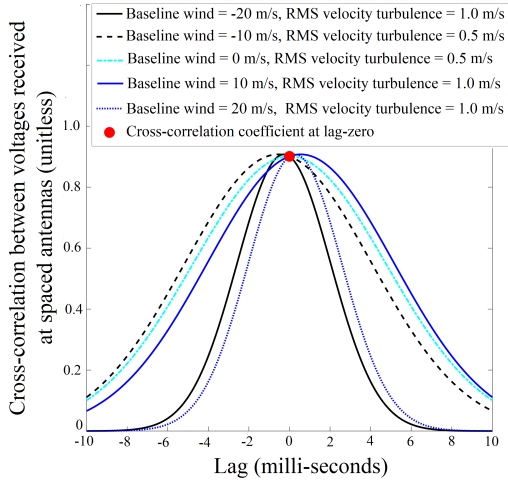


Fig. 5: Illustration of the concept for spaced antenna baseline measurement. Note that the magnitude of the cross-correlation  $\gamma$  is the same irrespective of wind-speed. A one-way antenna beamwidth of 2.6 degrees and a baseline of 8 cm were assumed.

Spaced-antenna retrievals of baseline wind are based on a model for the correlation between received voltages. Herein, we exploit this same correlation function model to assess the baseline of the implemented spaced-antenna system. Fig. 5 shows that the cross-correlation coefficient at zero-lag is invariant of wind-field statistics. As the baseline wind and RMS velocity turbulence change, we see that the cross-correlation at zero-lag remains fixed while the peak and width of the correlation function change. Based on this property of a fixed cross-correlation coefficient at lag-zero, an algorithm to derive baselines for spaced-antenna systems follows -

- 1) Measure beamwidth for each beam location using far-field methods. Denote each measurement of the equivalent beamwidth as  $\hat{\phi}_e$  (in radians). This is related to the beamwidths of the left and right monostatic combinations by the relationship  $\hat{\phi}_e^2 = \frac{2}{\frac{1}{\sigma_{e\phi TR_L}^2} + \frac{1}{\sigma_{e\phi TR_R}^2}}$ . Here,  $\sigma_{e\phi TR_L}$  and  $\sigma_{e\phi TR_R}$  are second central moments of the left and right spaced-antenna beams respectively.
- 2) On precipitation echoes, estimate the cross-correlation magnitude at lag-zero for each beam location. Denote each such measurement as  $|\hat{\gamma}(\Delta x, 0)|$ .
- 3) For each beam location, retrieve the baseline from the relationship [11]

$$\Delta \hat{x} = \sqrt{\frac{-\ln|\hat{\gamma}(\Delta x, 0)|16\ln(2)}{2k^2\hat{\phi}_e^2}}. \quad (1)$$

Here,  $k$  is the radar wavenumber. Other variables have been defined earlier.

Fig. 6 shows results that measure the relative phase-center displacement of the monostatic spaced-antenna combinations.

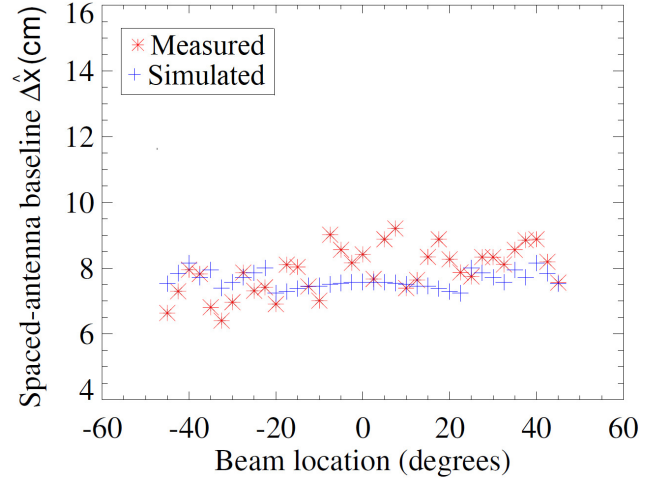


Fig. 6: Synthesized spaced-antenna baselines for the 2.6 degree equivalent one-way beamwidth design. The good agreement between simulated baselines and measured baselines validates the implementation of this design.

The top panel in Fig. 6 compares measurements of cross-correlation magnitudes at zero-lag to simulated values. For this figure, the simulations employ the measured beamwidths in Fig. 3. The cross-correlation coefficient estimates were obtained using the spectral moments method described in [7] because it allowed for simple filtering of ground clutter. The following quality control metrics were used to selectively average the cross-correlation coefficient for a given beam location -

- 1) Spectrum with greater than 1 m/s. Since the baseline measurement algorithm employed requires volume scattering, this threshold removes ground clutter artifacts.
- 2) SNR greater than 20 dB. This threshold effectively removes effects of noise “spikes” of the cross-correlation at zero-lag because of elements common to both apertures.

The bottom panel in Fig. 6 compares baseline measurements to simulated values. The agreement of the measured baselines with expected values effectively validates the algorithm for baseline measurement. Note that the good performance of the algorithm was a direct result of the high cross-function coefficient at lag-zero. Had wider beams or longer baselines been employed, the fidelity of the baselines measured with this algorithm would have degraded.

### C. Beam squint measurements

Fig. 7 shows a comparison in beam squinting errors for the implemented broadside spaced-antenna systems. Specifically, short baselines have little differential squint between the left and right spaced-antenna systems. This is because of element level errors are retained on spaced-antenna systems with significant overlap. But the differential beam squint errors show a systematic increase as a function of baseline. This is because systematic errors such as incorrect inter-element spacing knowledge become more pronounced as the baseline increases and contribute more significantly to differential beam squint between the left and right spaced antenna systems.



Further, we note that it suffices if we evaluate differential beam squint errors between the left and right spaced-antenna systems alone. Relative squints between the Tx/Rx patterns reduce the system SNR but do not have a direct impact on the synthesized baselines. We therefore do not consider Tx/Rx squint errors in this work because one may compensate for the SNR loss by other means.

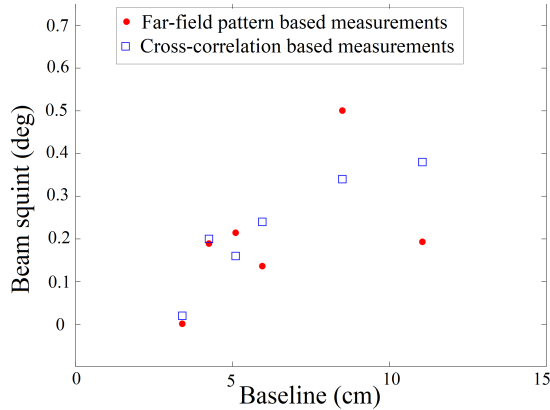


Fig. 7: Difference between beam pointing angles of the left and right spaced antenna systems. Both far-field pattern measurements and the cross-correlation based method show that spaced antenna systems with short baselines and largest number of overlapping elements have the least beam squint.

#### IV. SUMMARY

To date, literature on adapting the SA concept to microwave weather radars has been largely focussed on theoretical modelling and simulation based studies. The lack of success in spaced-antenna weather radar implementations to date may, in part, be attributed to difficulty in optimizing system design. In this work, we investigated aperture synthesis for an X-band SA weather radar using a flexible active phased array concept. Segmenting an active array face into sub-arrays with displaced phase-centers, a variety of spaced-antenna weather radar implementations were examined. Far field antenna patterns of these spaced-antenna systems were measured by stepping through the beams to be evaluated while slowly mechanically scanning the antenna array face past a beacon. Statistics of real data collected with the spaced-antenna systems were found to be qualitatively consistent with the antenna pattern measurements.

The figures of merit used to evaluate errors in aperture synthesis were beamwidth, baseline and relative squint between the left/right spaced-antenna systems. In examining beamwidth and beam squint errors relative to simulated expectations, antenna far-field pattern measurements were of primary importance. The reasonable agreement of simulated results with measurements validated the simulation methodology employed herein. Using these simulated expectations as a prognostic, real data collected with the X-band phased-array was used to demonstrate a novel method to measure the spaced-antenna baseline based on received echo statistics. This algorithm exploited the invariance of the cross-correlation function at

lag-zero to meteorological parameters such as wind-speed and RMS velocity turbulence. By taking advantage of prior knowledge of radar wavenumber and beamwidth, this technique allows for “in-place” calibration of spaced antenna systems and can be used to compensate for inevitable T/R module failures as they occur. Existing spaced antenna profilers such as the Multiple Antenna Profiler (MAPR) [2] and the Jicamarca radio observatory [1] may readily incorporate this method. Finally, we find that highly overlapping spaced-antenna arrays were most immune to relative beam squint errors between the left and right SA systems. This is because element level errors are retained on the left and right spaced antenna systems, thereby minimizing the impact on differential beam squint. Since the use of apertures with non-overlapping elements gave rise to beamforming errors, it limited the flexibility offered by active phased-array technology for synthesizing spaced-antenna systems. But to the extent possible, spaced-antenna aperture calibration measurements using the procedure developed in this work can be used to correct retrievals of cross-beam wind.

#### REFERENCES

- [1] J. Chau, R. J. Doviak, A. Muschinski, and C. Holloway, “Lower atmospheric measurements of turbulence and characteristics of bragg scatterers using the jicamarca vhf radar,” *Radio Sci.*, vol. 39, pp. 179–193, 2000.
- [2] S. A. Cohn, W. O. J. Brown, C. L. Martin, M. E. Susedik, G. MacLean, and D. B. Parsons, “Clear air boundary layer spaced antenna wind measurement with the multiple antenna profiler (MAPR),” *Ann. Geophys.*, vol. 19, no. 8, pp. 845–854, 2001.
- [3] B. H. Briggs, G. J. Phillips, and D. H. Shinn, “The analysis of observations on spaced receivers of the fading of radio signals,” *Proc. Phys. Soc. London, B*, vol. 63, pp. 106–121, 1950.
- [4] A. Pazmany, H. B. Bluestein, M. M. French, and S. Frasier, “Observations of the two-dimensional wind field in severe convective storms using a mobile X-band Doppler radar with a spaced antenna,” in *22nd Conference on Severe Local Storms*. Hyannis, MA: AMS, 2004, p. P7.3.
- [5] G. Zhang and R. J. Doviak, “Spaced-antenna interferometry to measure crossbeam wind, shear and turbulence: Theory and formulation,” *J. Atmos. Oceanic. Tech.*, vol. 24, pp. 791–805, 2007.
- [6] —, “Spaced-antenna interferometry to locate sub-volume inhomogeneities of reflectivity: An analogy with monopulse radar,” *J. Atmos. Oceanic. Tech.*, vol. 21, pp. 1921–1938, 2008.
- [7] V. Venkatesh and S. Frasier, “Simulation of spaced-antenna wind retrieval performance for an x-band phased-array weather radar,” *J. Atmos. Oceanic. Tech.*, p. In press, 2012.
- [8] K. Orzel and S. Frasier, “Weather observation by an electronically scanned dual-polarization phase-tilt radar,” *IEEE Trans. Geoscience Remote Sensing*, vol. 56.5, pp. 2722–2734, 2018.
- [9] J. L. Salazar, E. Knapp, and D. J. McLaughlin, “Dual-polarization performance of the phase-tilt antenna array in a casa dense network radar,” in *Int’l. Geosci. & Remote Sensing Symposium*. Honolulu, HI: IEEE, 2010.
- [10] R. Mailloux, *Phased Array Antenna Handbook*, 2nd ed. Artech House, 2005.
- [11] V. Venkatesh, “Spaced-antenna wind estimation using an x-band active phased array weather radar,” Ph.D. dissertation, University Of Massachusetts at Amherst, 2013.